Electronic structure of the hollow-cage M_8X_{12} clusters

L. Lou, T. Guo, P. Nordlander, and R. E. Smalley
Rice Quantum Institute and Departments of Chemistry and Physics, Rice University, Houston, Texas 77251-1892

(Received 14 April 1993; accepted 23 June 1993)

The electronic structure of recently discovered hollow-cage molecule Ti_8C_{12} has been calculated and compared to similarly shaped hypothetical molecules M_8X_{12} (M=metal and X=B, C, or N). The cohesion of the cage is related to the σ-bonding between M–X arising from *d–sp* hybridization. It is also shown that the cage can become electronically closed shell with all the valence electrons paired when the carbon is replaced by boron or nitrogen, e.g., in the formula of Sc_8B_{12}.

I. INTRODUCTION

The exceptional abundance of M_8C_{12} (M=Ti, V, Zr, and Hf) clusters in mass spectrometer recently observed by Castleman and co-workers[1,2] has stimulated several theoretical investigations of the electronic structure and the bonding mechanisms of these species, using either many-electron wave function methods[3–5] or density-functional methods.[6–9] The focus has been on the M_8C_{12} clusters with M being transition metal elements on the left side of the periodic table, e.g., Sc, Ti, and V. The atomic arrangement is assumed to be a hollow cage in T_h symmetry in which the metal elements occupy the eight unique positions, each connecting to three symmetrically equivalent carbon atoms.

A common feature of these carbon transition-metal clusters is the dense population of valence orbitals with significant *d* character in the energy regions near the "Fermi" level. This open-shell-type electronic structure is the reason why these species easily form compounds with NH_3 and H_2O. The existence of unsaturated valence orbitals causes the metal sites to be reactive. From an experimental point of view, it would be desirable to have closed-shell singlet species with the closing electron pair well separated in energy from the next unoccupied orbital level: Clusters having this type of electronic structure will be easier to prepare in pure form and can be handled more like an ordinary molecule.

Since each atom in the T_h symmetry arrangement connects to three neighbors, closed-shell singlet configuration may be constructed from trivalent atoms. We have chosen two combinations of elements Sc/B and Al/N and studied the corresponding clusters Sc_8B_{12} and Al_8N_{12} assuming the same T_h symmetry arrangements.

When atoms of different valence replace the original transition metal and carbon atoms in the M_8C_{12} formula, the question about structural stability of the T_h cage arises. The observed M_8C_{12} clusters all have transition metal elements of less than half filled *d* shell. In order to investigate whether elements outside of this region in the periodic table can form stable cagelike clusters, two nontransition metal elements Ca and Zn have been chosen to substitute for M in M_8C_{12}. Since calcium has a closed 4*s* shell and empty 3*d* shell and zinc has both 4*s* and 3*d* shells closed, the corresponding clusters Ca_8C_{12} and Zn_8C_{12} can be considered as extreme cases of the family of M_8C_{12} clusters with M being any element between Ca and Zn.

Since these clusters contain other first-row elements in the position of carbon, and metal elements from the parts of the Periodic Table other than the early *d*-metal block, a modified formula M_8X_{12} will be used to reflect these changes. The use of this slightly changed formula gives more room for choosing elements to fill the 20 vertex positions of a T_h dodecahedron.

II. COMPUTATION

The electronic and geometric structures of the clusters are calculated using a recently developed *ab initio* density-functional method.[10] Numerically tabulated atomic orbitals are used to expand the wave functions. The matrix elements and the effective potentials in the Kohn–Sham formalism[11] are evaluated on a grid of sampling points using the numerical techniques introduced (and described in detail) by Becke[12] and Delley.[13] For each atom, an all-electron polarized double-numerical basis set[14] is used. Typically, such a basis set contains all the occupied atomic orbitals of the neutral atom and the valence orbitals of the doubly charged ionic state. A single polarization function is used for each element, which can be either *p* type or *d* type depending on the last occupied shell of that element. The exchange-correlation functionals of Hedin and Lundqvist[15] and the parameterization by von Barth and Hedin[16] are used in the generation of atomic orbitals as basis functions and in the calculation of M_8X_{12} clusters. Previous calculations showed that numerical basis sets of this size can yield satisfactory ground state parameters for small molecules and clusters.[17] Due to the precise nature of the numerical functions, the basis sets so constructed have higher quality than similarly sized double-ζ type bases. The numerical scheme employed in this calculation has been tested for a number of typical molecules and small clusters against a commercial version of DMol (Biosym Technologies, San Diego, CA) and very similar results have been obtained by the two schemes (see, e.g., Ref. 17).

To facilitate the convergence of SCF iteration procedure, orbitals near the Fermi level are allowed to take fractional occupation numbers according to the Fermi distribution of a finite temperature of about 30 K.

 0021-9606/93/99(7)/5301/5/$6.00

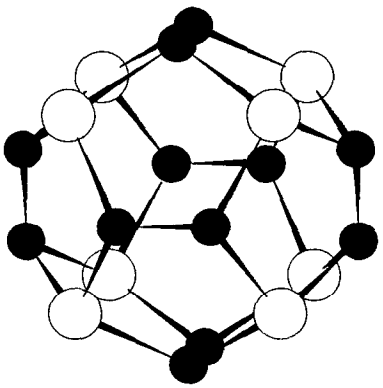

FIG. 1. A dodecahedron of T_h symmetry. The M_8X_{12} clusters are assumed to have this cagelike arrangement. The metal atoms M occupy the eight unique positions (open circles), each connecting to three symmetrically equivalent X atoms (shaded circles).

The cluster geometry is relaxed by minimizing the analytically calculated energy gradients.[18,19] The relaxation is performed within the D_{2h} symmetry and terminated when the maximum gradients fall below 0.001 a.u. The small distortion from the T_h symmetry in the final geometry is neglected in accordance with the use of a finite-temperature scheme for orbital population.

III. RESULTS

The calculated geometric and electronic properties of the five clusters Ca_8C_{12}, Ti_8C_{12}, Zn_8C_{12}, Sc_8B_{12}, and Al_8N_{12} are listed in Table I. The Mulliken population (projected on the local atomic orbitals of different angular momentum) and the gross atomic charge of these clusters are given in Table II.

Figures 2 and 4 show the energy resolved populations for the overlapping atomic orbitals[20] centered at a metal (M) atom and a neighboring X-type atom (X=B, C, or N). These energy resolved populations are partial sums of the density matrix for the elements corresponding to the overlapping atomic orbitals. Summation of these matrix elements from the lowest energy upwards to the Fermi level gives the Mulliken overlap populations. The energy range chosen for these figures is sufficiently wide to include major bonding and antibonding contributions from the valence electrons.

TABLE I. Calculated ground state properties of dodecahedral clusters M_8X_{12}. The binding energy E_0 is in eV/atom and the bond length r and shell radius ρ are in Å.

M_8X_{12}	Ca_8C_{12}	Ti_8C_{12}	Zn_8C_{12}	Sc_8B_{12}	Al_8N_{12}
E_b	5.25	6.64	4.65	5.05	4.60
r(X–X)	1.28	1.40	1.28	1.51	1.55
r(X–M)	2.41	1.97	2.03	2.26	1.84
r(M–M)	3.26	3.04	2.96	3.21	2.70
ρ(X)	3.17	2.64	3.17	3.04	2.57
ρ(M)	2.83	2.57	2.83	2.78	2.34

TABLE II. The Mulliken population (condensed to s, p, and d atomic-orbital types) and gross atoms charge (Q) of the M_8X_{12} clusters. The valence configuration of each M or X type atom is enclosed in parentheses.

M_8X_{12}	Ca_8C_{12}	Ti_8C_{12}	Zn_8C_{12}	Sc_8B_{12}	Al_8N_{12}
M	Ca(d^0s^2)	Ti(d^2s^2)	Zn($d^{10}s^2$)	Sc(d^1s^2)	Al(s^2p^1)
s	0.36	0.18	0.77	0.28	0.61
p	0.23	0.31	0.70	0.42	1.03
d	0.53	2.77	10.03	1.60	0.54
Q	0.89	0.75	0.50	0.70	0.83
X	C(s^2p^2)	C(s^2p^2)	C(s^2p^2)	B(s^2p^1)	N(s^2p^3)
s	1.52	1.47	1.43	1.36	1.61
p	3.01	2.94	2.82	2.08	3.86
d	0.06	0.09	0.08	0.04	0.09
Q	−0.59	−0.50	−0.33	−0.47	−0.55

Figures 3 and 5 show the deformation charge densities at two different cutting planes. The deformation density of a cluster is defined as the difference between the cluster charge density and the superposition of atomic charge densities. The density difference illustrates, approximately, the charge transfer associated with the formation of a bond between certain atoms such as titanium and carbon within a cage arrangement.

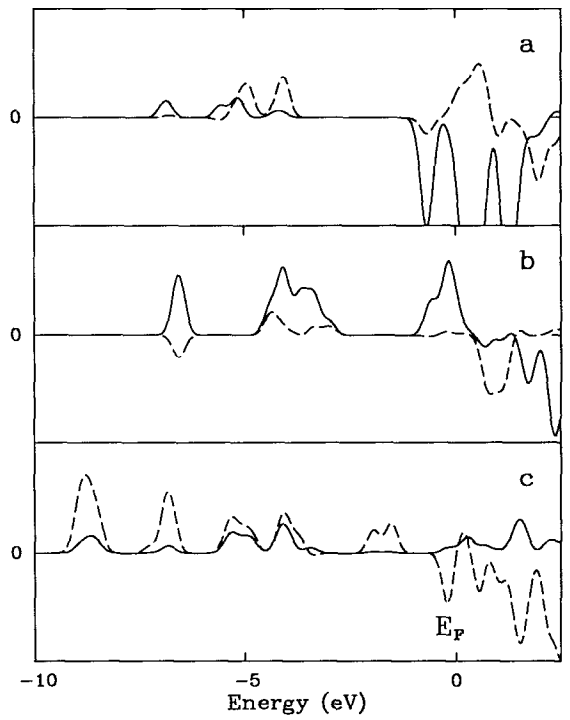

FIG. 2. Energy resolved populations for overlapping atomic orbitals. The overlap is between the atomic orbitals centered at a metal atom (M), and a neighboring C atom. The discrete states have been self-convoluted with a Gaussian of width 0.2 eV. The solid curves represent the part due to metal d orbitals and the dashed curves represent the part due to metal s and p orbitals. Note that the overlap population includes contributions of *all* the atomic orbitals attached to the C atom. The sign of the areas beneath each curve indicates bonding (positive sign) or antibonding (negative sign) characters of the overlapping orbitals. The Fermi level for each cluster has been aligned at zero. (a) Ca_8C_{12}; (b) Ti_8C_{12}; (c) Zn_8C_{12}.

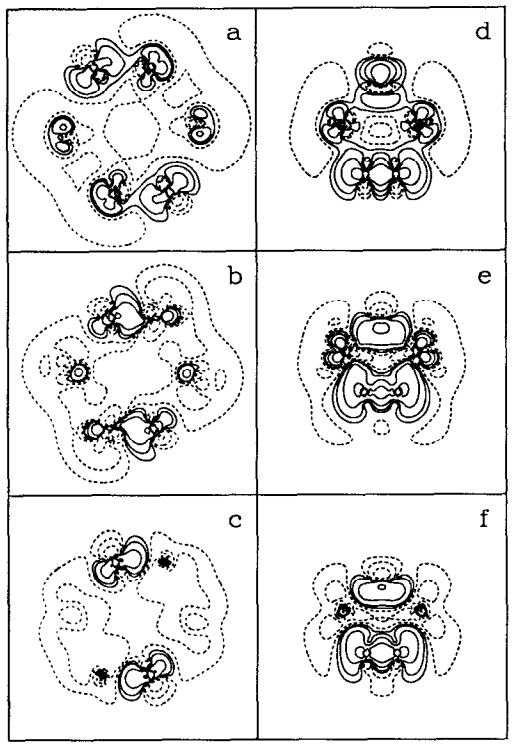

FIG. 3. Deformation charge density contours (see the text for the definition). The contours in the left panel (a)–(c) are drawn for the plane which passes through two M–C bonds related by the inversion center and cuts other two M–C bonds. The contours in the right panel (d)–(f) are drawn for the plane passing through two M atoms and two C atoms within a pentagonal ring. The third C atom is beneath the plane. The clusters are in a distorted dodecahedral form such that the five-member rings are not planar. The side length of each subplot is 20 by 20 in atomic units (a_0). The contour levels are 3, 9, 27, and 81×0.0005 a_0^{-3}. The electrons are concentrated at carbon sites (solid lines) and depleted from the metal sites (dashed lines). (a), (d) Ca_8C_{12}; (b), (e) Ti_8C_{12}; (c), (f) Zn_8C_{12}.

A. Ti_8C_{12}, Ca_8C_{12}, and Zn_8C_{12}

The Ti_8C_{12} cluster has received the most attention so far. This cluster has an open-shell ground state in a cage-like arrangement of T_h symmetry. The highest occupied molecular orbital (HOMO) t_g is only partially filled (with two spin-aligned electrons), resulting in a triplet state ^3T_g. Due to the dense population of orbitals near the HOMO level, however, low-lying excited states with different orbital configurations may exist for this cluster. Figure 2(b) shows that the dense band around the HOMO level is mainly of *d* character and of bonding nature. The titanium *d* electrons can form bonds with neighboring carbon through *dsp* hybridization.

The C–C bond length of 1.40 Å for Ti_8C_{12} is typical for a carbon–carbon double bond. The Ti–C bond distance in Ti_8C_{12} is 1.97 Å. This value lies between the corresponding values of TiC diatomic (1.60 Å, obtained by using the same basis set as in the cluster calculation) and the TiC solid [2.16 Å (Ref. 21)], indicating a relatively strong connection between Ti and C in the T_h-cage arrangement of Ti_8C_{12} cluster.

The third column in Table II gives the Mulliken populations over the *s*-, *p*-, and *d*-type atomic orbitals attached to a titanium and to a carbon. It can be seen that the populations of *p* and *d* orbitals around the Ti atoms are significantly increased. The increased population of titanium *p* and *d* orbitals is consistent with the picture that titanium and carbon form σ bonds through *dsp* hybridization. Since the charges are strongly polarized towards carbon in the titanium–carbon bond, the population of *s* orbitals both at the titanium sites and at the carbon sites are decreased.

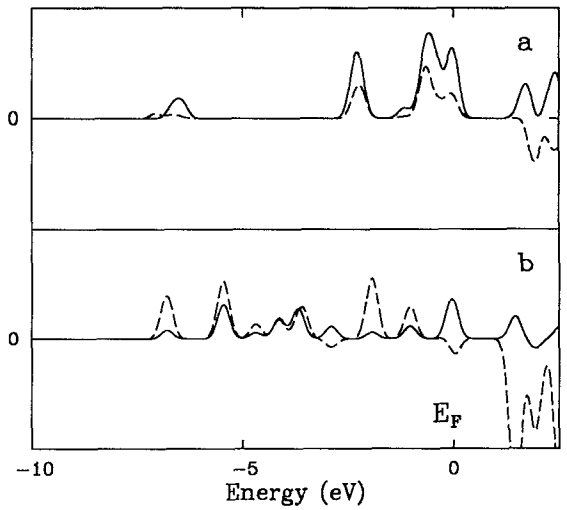

FIG. 4. Density of states for overlapping atomic orbitals. The organization of the figure is as in Fig. 2. (a) Sc_8B_{12}; (b) Al_8N_{12}.

The deformation charge densities provide further evidence for the existence of strongly polarized Ti–C bonds. As shown in Figs. 3(b) and 3(e), the solid contour lines, which represent a charge buildup, extend from carbon towards titanium. Alongside the line joining a titanium and a neighboring carbon, there are small charge depletion areas represented by dashed contour lines, indicating charge

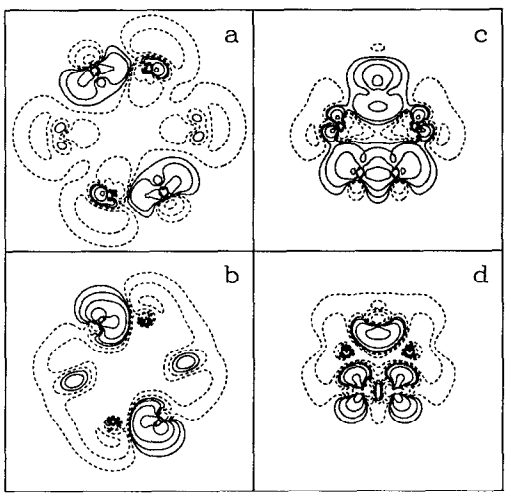

FIG. 5. Deformation charge density contours for Sc_8B_{12} and Al_8N_{12}. The organization of the figure is as in Fig. 3. (a), (c) Sc_8B_{12}; (b), (d) Al_8N_{12}.

TABLE III. Binding energies E_b (in eV) of diatomics MX at the bond distance R_{M-X} (in Å) in the corresponding M_8X_{12} clusters.

MX	CaC	TiC	ZnC	ScB	AlN
State	$^3\Sigma^-$	$^1\Sigma^+$	$^1\Sigma^+$	$^3\Sigma^-$	$^2\Pi$
E_b	2.82	4.90	1.84	3.07	3.24
R_{M-X}	2.41	1.97	2.03	2.26	1.84

transfers from Ti towards C. Note that the increment of contour levels is logarithmic.

The other two carbon-metal clusters, Ca_8C_{12} and Zn_8C_{12} also have open-shell electronic structure. In both cases, the HOMOs are partially occupied resulting in a ^3T_g state. However, there is some difference in the density of states between the two clusters. For Ca_8C_{12}, the HOMO is near the bottom of a band largely composed of antibonding *d* orbitals. Whereas the partially occupied HOMO of Zn_8C_{12} is separated from above and beneath by 2–3 eV.

The difference between Ca_8C_{12} and Ti_8C_{12} can be best illustrated through the contribution of *d* orbitals to the metal–carbon bonding. As shown in Figs. 2(a) and 2(b), the calcium *d* orbitals have both bonding and antibonding contributions while the titanium–carbon bonding is predominantly of *d* character. The Ca–C bonds are mainly of *sp* character and more ionic with the Ti–C bonds.

The bonding in the Zn_8C_{12} is also of *sp* type. The filled *d* shell of zinc ion polarizes but does not directly contribute to the Zn–C bonding. This is illustrated by the almost unchanged *d*-orbital populations in Table II and the very rounded shape of deformation density contours outside the zinc ion core as shown in Figs. 3(c) and 3(f). Correspondingly, the Zn–C bond is less polarized than the Ti–C and Ca–C bonds.

The weakened metal–carbon bonding in Ca_8C_{12} and Zn_8C_{12} allows the carbon atoms in the cage to form shorter and stronger bonds. The C–C distance is 1.28 Å in both clusters, which is 0.12 Å shorter than that in Ti_8C_{12}. This bond length is about the same as the bond length of C_2^{-1} anion (1.28 Å, obtained by using the same basis set for carbon as in the cluster calculation). The existence of strongly coupled C–C pairs in the cage structure of these two clusters is manifested by the density contours in Figs. 3(d) and 3(f). The charge buildup around the C–C pairs shows clearly the characters of π interactions.

Given the strong contraction between the strengths of carbon–carbon bonds and metal–carbon bonds, the present T_h-cage arrangement might not be optimal for Ca_8C_{12} and Zn_8C_{12}. Instead, these two carbon *s*-metal clusters may prefer different stoichiometric compositions and noncage structures as suggested by a recent experiment on carbon copper cluster cations,[22] in which the 8–12 magic number does not appear.

In contrast to the weak bonds formed between carbon and *s*-metal atoms in a cage arrangement, the metal–carbon bonds in Ti_8C_{12} are strengthened by the *dsp* hybridization. The hybrid orbitals can form optimal σ bonds between adjacent Ti and C. Table III lists the binding energies of various diatomics at appropriate inter-atomic distances. The diatomic binding energies can be used to estimate the bond strength in the corresponding cage clusters. For example, the TiC diatomic at bond distance 1.4 Å has a bonding energy of 4.9 eV, or 2.5 eV/atom. This value is much larger than the corresponding values of CaC and ZnC diatomics.

B. Sc_8B_{12} and Al_8N_{12}

The Sc_8B_{12} cluster has a closed-shell singlet ground state. The calculated HOMO-LUMO gap, 1.68 eV, is substantial. A similar result is obtained using another SCF method.[23] Both Sc and B are trivalent. The valence electrons in this cluster are paired, one pair for each bond. Since there is no unpaired electrons left, this cluster is expected to be chemically more stable than the typical carbon transition-metal cluster Ti_8C_{12} which has a vanishing HOMO-LUMO gap.

The Sc_8B_{12} cluster has a binding energy 5.05 eV/atom. The direct comparison with Ti_8C_{12} show a decrease in binding energy about 1.6 eV/atom. However, the diatomic binding energy values in Table III provide another way to estimate the structural stability of this cluster. The difference between the Ti–C bonds and the Sc–B bonds at appropriate distances is 1.8 eV per bond or 2.7 eV per atom. Not including the difference between the strengths of C–C bonds and B–B bonds, this M–X bond energy difference alone is already much larger than the direct binding energy difference 1.6 eV/atom between Ti_8C_{12} and Sc_8B_{12}. The net gain in energy is more than 1 eV/atom. The bonding between Sc and B in the cage arrangement is rather strong.

The involvement of the *d* orbitals in the bonding between Sc–B is illustrated in Fig. 4(a). The overlapping orbitals between Sc and B is predominantly of *d* character, similar to the case of Ti_8C_{12}. The bonding between B–B is also strengthened by the *sp* hybridization. This result is supported by the Mulliken population in Table II and the deformation charge density in Figs. 5(a) and 5(c).

The Al_8N_{12} cluster is also of closed-shell type. The N–N pairs are singly bonded as are the B–B pairs in Sc_8B_{12}. The separation between HOMO-LUMO for this cluster is 1.46 eV. The N–N bond length in Al_8N_{12} is also close to the B–B bond length in Sc_8B_{12}. However, the similarity between the two clusters actually stops here; significant difference can be found from the comparison of other attributes. For example, the aluminum ions form shorter bonds with the neighboring nitrogen, resulting in shorter Al–Al distances and larger Coulomb repulsions between Al ions.

The difference in Mulliken population between Al_8N_{12} and Sc_8B_{12} is also significant. The effects of Al *s*-electron polarization is mainly to populate the local *d* orbitals and the *p* orbitals around neighboring nitrogen anions. The number of *p*-type electrons near Al atoms remains basically unchanged. The Al–N interaction contains not only contributions from *sp* hybridization but also contributions from the populated Al *d* orbitals. This can be seen in Fig. 4(b), where both the *d* orbitals and the *sp* orbitals of Al have bonding overlap with the orbitals from a neighboring N atom. The positive but relatively small areas under the solid-line curve in Fig. 4(b) suggest that the *d*-orbital con-

tribution to the Al–N bonding be moderate, as compared to the contribution of *d* orbitals in Ti–C and Sc–B bonding.

The large charge transfer from Al to N as indicated by the gross atomic charge (see Table II) is also reflected in the deformation density contours in Figs. 3(b) and 3(d). On the other hand, similarities can be found between the density contours of Sc_8B_{12} [Figs. 3(a) and 3(c)] and Ti_8C_{12} [Figs. 2(b) and 2(e)].

The calculated binding energy of Al_8N_{12} is 4.6 eV/atom. As a comparison, the total binding energy of ten N_2 diatomics is 5.4 eV/atom. This indicates that the formation of the Al_8N_{12} cage structure is energetically unfavored. The very enlongated N–N bond makes the cage arrangement less competitive than the mechanism of forming separate N_2 dimers.

IV. DISCUSSION

In all the five M_8X_{12} clusters studied, the X–X pairs are characterized by the formation of strong π bonds. The population of *p* orbitals around each X atom has increased by nearly one electron. This extra charge comes partly from the local *s* orbitals and partly from the neighboring metal sites. The increased population of the local *p* orbitals enhances the π bonding. This feature would be lost if identical X atoms were placed in the eight metal positions to form a homogeneous cage cluster.

The bonding between M–X is crucial to the cohesion of the cage structure. Since the X–X pairs are very strongly coupled, there is a potential for these X_2 units to break apart from the cage network if the M–X bonding is weak. The formation of the *dsp* hybrid at the metal sites provides the necessary flexibility to form direct and strong σ type bonds with the neighboring X atoms and therefore enhances the cohesion of the cage.[3] Correlations between the M–X bond strength and the *d*-orbital involvement in the M–X bonding exist.

The position of Ca and Zn in the periodic table is the main reason for these two metal elements to be chosen as substitutions for the *d* metals in the formula M_8X_{12}. This choice is rather arbitrary. Other metal elements may well be chosen for better reasons, e.g., the last element of the 3*d* series, Cu, the main group *p*-metal Al, and the s^2p^2 isoelectronic element Si.[6] The possibilities of different combinations of elements in the general formula M_8X_{12} have not yet been systematically studied, at least from the theoretical side.

The transition metal elements such as Sc and Ti can bond strongly with first row elements B, C, or N. The corresponding cage clusters tend to have high binding energy. The Sc_8B_{12} cluster is of particular interest. Due to its closed-shell electronic structure, the T_h isomer of this cluster may be actually stable against residual molecules such as H_2O and NH_3 and may survive for a long time without forming compounds. In addition, the high vaporization temperature of scandium and boron makes it relatively easy to prepare the sources for a cluster-beam experiment. Experiment for observing boron transition-metal clusters is in progress.

V. CONCLUSIONS

The electronic structure of cagelike M_8X_{12} clusters, with M being *d*-metal and *sp*-metal elements and X being B, C, and N, has been studied using a local-spin-density method and double-numerical plus polarization bases. It is shown that the transition metal elements such as Sc and Ti can form strong σ bonds with carbon within a cage arrangement, while a similar cage arrangement might not be optimal for other metal elements such as Ca and Zn. It is also shown that the cagelike clusters can have very different electronic properties if appropriate elements are in the positions of titanium and carbon. For example, Sc_8B_{12} has a closed-shell singlet ground state with a substantial HOMO-LUMO gap and therefore should be chemically more stable than its carbon transition-metal analogies.

ACKNOWLEDGMENTS

The authors would like to thank Dr. Bruce Johnson for coordinating the computer resources at Chemistry Department of Rice University. This research was supported by the U.S. Department of Energy, Division of Chemical Science, and the Robett A. Welch Foundation.

[1] B. Guo, K. Kerns, and A. Castleman, Science **255**, 1411 (1992).
[2] B. Guo, S. Wei, J. Purnell, S. Buzza, and A. Castleman, Science **256**, 515 (1992).
[3] Z. Lin and M. B. Hall, J. Am. Chem. Soc. **114**, 10054 (1992).
[4] M.-M. Rhomer, P. de Vaal, and M. Benard, J. Am. Chem. Soc. **114**, 9696 (1992).
[5] P. J. Hay, J. Phys. Chem. **97**, 3081 (1992).
[6] R. W. Grimes and J. D. Gale, J. Chem. Soc., Chem. Commun. September, 1222 (1992).
[7] B. Reddy, S. Khanna, and P. Jena, Science **258**, 1640 (1992).
[8] T. T. Rantala, D. A. Jelski, J. R. Browser, X. Xia, and T. F. George, Z. Phys. D (in press).
[9] M. Methfessel, M. van Schilfgaarde, and M. Scheffler, Phys. Rev. Lett. **70**, 29 (1993).
[10] L. Lou (unpublished).
[11] R. O. Jones and O. Gunnarsson, Rev. Mod. Phys. **61**, 689 (1989).
[12] A. D. Becke, J. Chem. Phys. **88**, 2547 (1988).
[13] B. Delley, J. Chem. Phys. **92**, 508 (1990).
[14] B. Delley, in *Density Functional Methods in Chemistry*, edited by J. Labanowski and J. Andzelm (Springer, Berlin, 1991).
[15] L. Hedin and B. I. Lundqvist, J. Phys. C **4**, 2064 (1971).
[16] U. v. Barth and L. Hedin, J. Phys. C **5**, 1629 (1972).
[17] L. Lou, P. Nordlander, and R. E. Smalley, J. Chem. Phys. **97**, 1858 (1992).
[18] B. Delley, J. Chem. Phys. **94**, 7245 (1991).
[19] L. Versluis and T. Ziegler, J. Chem. Phys. **88**, 322 (1988).
[20] R. Hoffmann and C. Zheng, in *Proc. NATO Advanced Research Workshop and 40th Intern. Meeting of the Societe du Chimie Physique, Strasbourg, France, 16–20 September 1985*, edited by A. Veillard (Reidel, Dordrecht, 1986), p. 425.
[21] *A Handbook of Lattice Spacings and Structures of Metals and Alloys*, edited by W. Pearson, Pergamon, New York, 1967.
[22] Y. Yamada and A. Castleman, Chem. Phys. Lett. **204**, 133 (1993).
[23] G. Guo, G. Odom, G. Scuseria, and R. Smalley (unpublished).